Coupling vortex dynamics with collective excitations in Bose-Einstein condensates

R. P. Teles, V. S. Bagnato, and F. E. A. dos Santos
Instituto de Física de São Carlos, USP, Caixa Postal 369, 13560-970 São Carlos, São Paulo, Brazil
(Received 10 June 2013; published 13 November 2013)

Here we analyze the collective excitations as well as the expansion of a trapped Bose-Einstein condensate with a vortex line at its center. To this end, we propose a variational method where the variational parameters have to be carefully chosen in order to produce reliable results. Our variational calculations agree with numerical simulations of the Gross-Pitaevskii equation. The system considered here turns out to exhibit four collective modes of which only three can be observed at a time depending on the trap anisotropy. We also demonstrate that these collective modes can be excited using well established experimental methods such as modulation of the s-wave scattering length.

DOI: 10.1103/PhysRevA.88.053613 PACS number(s): 03.75.Kk

I. INTRODUCTION

In this work, we are interested in the dynamics of a trapped Bose-Einstein condensate (BEC) containing a line vortex at its center. Here we are particularly interested in obtaining the collective oscillation modes of the system which couples the vortex-core oscillations with the oscillations of the condensate external dimensions. The interest in this problem is motivated by the fact that these oscillations can be measured in the laboratory by moving the atomic cloud out of its equilibrium configuration by using the Feshbach resonance in order to modulate the scattering length [1–5]. These oscillations are also studied in other physical systems such as two-species condensates [6], BCS-BEC crossover [7–9], and superfluid helium [10]. From the theoretical point of view, we are interested in how the size of the vortex core oscillates with respect to the external dimensions of the cloud. The mode with the smallest oscillation frequency is the quadrupole mode which occurs when the longitudinal and radial sizes of the condensate oscillate out of phase. The breathing mode requires more energy to be excited since the change in the density of the atomic cloud imposes a greater resistance against deviation from its equilibrium configuration than in the case of quadrupole excitations [11,12].

The frequency shifts of quadrupole oscillations due to the presence of a singly charged vortex have been analytically explored for positive scattering lengths using the sum-rule approach [13] as well as the effects of lower-dimensional geometry on the frequency splitting of quadrupole oscillations [14]. In Refs. [15–17], the dynamics of normal modes for a single vortex has been studied using hydrodynamic models, which focus on the vortex motion with respect to the center of mass of the condensate. This concept was also used in the case of multicomponent Bose-Einstein condensates [18] as well as in the description of the dynamics of single perturbed vortex lines [19].

Preliminary calculations using a variational approach with a Gaussian ansatz, which does not take into account the independent variation of the vortex-core size [3,6,18,20], shows a small shift in the frequencies of the aforementioned modes (Fig. 1). This shift has already been obtained via a hydrodynamic approximation in Refs. [12,21]. Thus we can expect the frequency of the monopole (breathing) mode to decrease while the quadrupole frequency increases in the presence of the vortex.

To calculate the dynamics of a vortex with charge ℓ in a more consistent way with the physical reality, which allows for the coupling between vortex core and the external dimensions of condensate, we could naively use a Thomas-Fermi (TF) ansatz [22],

$$\psi(\rho,\varphi,z,t) = A(t)\left[\frac{\rho^2}{\rho^2+\xi(t)^2}\right]^{\frac{\ell}{2}}\sqrt{1-\frac{\rho^2}{R_\rho(t)^2}-\frac{z^2}{R_z(t)^2}} \times \exp\left[i\ell\varphi + iB_\rho(t)\frac{\rho^2}{2} + iB_z(t)\frac{z^2}{2}\right], \quad (1)$$

where $R_\rho(t)$ and $R_z(t)$ are the respective condensate sizes in radial ($\hat{\rho}$) and axial ($\hat{z}$) directions, and $\xi(t)$ is the size of the vortex core. The variational parameters $B_\rho(t)$ and $B_z(t)$ specify the variations of the velocity field $\delta\mathbf{v} = B_\rho(t)\rho\hat{\rho} + B_z(t)z\hat{z}$. The next step is to calculate the equations of motion for the five variational parameters (ξ, R_ρ, R_z, B_ρ, B_z). Following these calculations, the equations of motion would be linearized. For the ansatz (1), this procedure leads to imaginary frequencies which are not consistent with the stable configuration where a singly charged ($\ell = 1$) vortex resides at the center of the condensate. The linearized equations of motion can be written in a matrix form according to

$$M\ddot{\delta} + V\delta = 0, \quad (2)$$

where δ is the vector with components given by deviations of the variational parameters from their equilibrium values. The solution of (2) is a linear combination of oscillatory modes whose oscillation frequencies obey the equation

$$\prod_n \varpi_n^2 = \det(M^{-1}V) = \frac{\det V}{\det M}. \quad (3)$$

In order to ensure that all frequencies ϖ_n are real, we must have $\det V/\det M > 0$. We know that $\det V > 0$ since its sign reflects the sign of the variational parameters, which represents the external dimensions of the cloud in the stationary situation. Therefore, $\det M$ must also be positive. In the case of ansatz (1) with $\ell = 1$, such conditions are not satisfied since $\det M < 0$, which indicates that there is something wrong with ansatz (1). In previous works [17,18,23,24], since the authors did not consider the size of the vortex core as a variational parameter, this problem did not appear. More specifically, the imaginary frequency problem arises for excitation modes where the

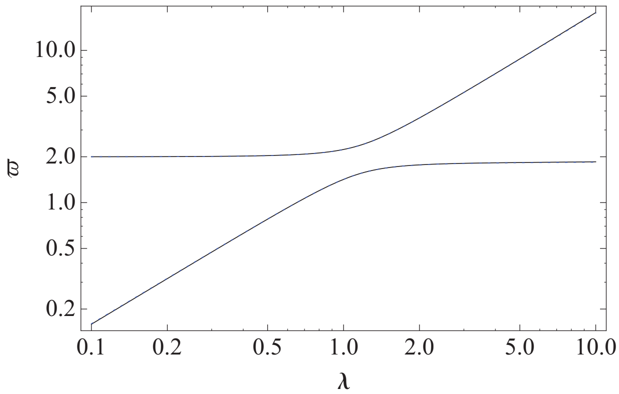

FIG. 1. (Color online) Oscillation frequencies from Gaussian ansatz without taking into account the independent variation of the vortex-core size. Upper lines correspond to the frequencies of the breathing mode as a function of the harmonic trap anisotropy, whereas lower lines represent the frequencies of the quadrupole mode. Solid (black) lines correspond to a vortex-free Gaussian profile, while dotted (blue) lines describe a profile with a singly charged vortex. Note that ϖ is normalized by the frequency of the radial direction ω_ρ.

vortex core and the external size of the cloud oscillate out of phase. This kind of motion generates a velocity field which changes the sign of its radial component as the distance to the vortex line is increased. Since the ansatz (1) describes only linear variations of this component, it is natural to expect nonphysical results in this case.

In Sec. II, the necessary requirements for the wave-function phase are discussed in order to give support to our variational method. Section III has the calculation based on the new ansatz and the corresponding equations of motion are obtained. The collective modes considering the coupling between vortex and atomic cloud are obtained via linearization of the equations of motion, thus resulting in new collective oscillations (Sec. IV). In Sec. V, we showed that such excitation modes can be excited using the scattering-length modulation. The free expansion was also calculated in order to complement a previous work [24]. Finally, Sec. VII contains the conclusions on our subject of study.

II. WAVE-FUNCTION PHASE

We start with the Lagrangian density,

$$\mathcal{L} = \frac{i\hbar}{2}\left(\psi^*\frac{\partial\psi}{\partial t} - \psi\frac{\partial\psi^*}{\partial t}\right) - \frac{\hbar^2}{2m}|\nabla\psi|^2 - V(\mathbf{r})|\psi|^2 - \frac{g}{2}|\psi|^4, \tag{4}$$

whose extremization leads to the Gross-Pitaevskii equation (GPE):

$$i\hbar\frac{\partial\psi}{\partial t} = \left[-\frac{\hbar^2}{2m}\nabla^2 + V(\mathbf{r}) + g|\psi|^2\right]\psi, \tag{5}$$

where $V(\mathbf{r}) = \frac{1}{2}m\omega_\rho^2(\rho^2 + \lambda^2 z^2)$ is an external potential, the trap anisotropy is $\lambda = \omega_z/\omega_\rho$, and g is the coupling constant. The complex field $\psi(\mathbf{r},t)$ can be written as an amplitude profile multiplied by a respective phase, as follows:

$$\psi(\mathbf{r},t) = f(w_l,\mathbf{r})e^{iS(\chi_l,\mathbf{r})}, \tag{6}$$

where

$$S(\chi_l,\mathbf{r}) = \ell\varphi + \sum_l \chi_l\phi_l(\mathbf{r}). \tag{7}$$

We denoted both, $w_l = w_l(t)$ and $\chi_l = \chi_l(t)$, respectively, as the amplitude and phase variational parameters. In principle, $\{\phi_l(\mathbf{r})\}$ should be a complete set of functions but, in our present approximation, we use only a representative incomplete set of functions. Substituting (6) and (7) into (4), the Lagrangian $L = \int \mathcal{L}\, d^3\mathbf{r}$ becomes

$$L = -\hbar\sum_l \dot{\chi}_l \int d^3\mathbf{r}\, f^2\phi_l - \frac{\hbar^2}{2m}\sum_l \chi_l^2 \int d^3\mathbf{r}\, f^2|\nabla\phi_l|^2 - \int d^3\mathbf{r}\left(\frac{\hbar^2}{2m}|\nabla f|^2 + Vf^2 + \frac{g}{2}f^4\right). \tag{8}$$

In order to account for the dynamics of all three variational parameters (R_ρ, R_z, and ξ) in f we include a variational phase which also contains three variational parameters. This way we chose the following trial function:

$$S(\rho,z,t) = \ell\varphi + B_\rho(t)\frac{\rho^2}{2} + C(t)\frac{\rho^4}{4} + B_z(t)\frac{z^2}{2}. \tag{9}$$

This allows the radial component of the velocity field to change its sign for different distances to the symmetry axis of the cloud. As the superfluid current is connected to the density variation, it is also desirable that both, amplitude and phase, have the same number of variational parameters. It is worth noticing that, in principle, any other ansatz allowing for such behavior of the velocity field would be equally valid. We chose to add an extra ρ^4 term to the wave-function phase due to its simplicity. The ansatz (9) also leads to linearized equations of motion (2) with det $M > 0$, which is consistent with the stability of the condensate with a singly charged vortex at its center.

III. EQUATIONS OF MOTION

Now we correct the Thomas-Fermi ansatz according to the discussion in Sec. II. This leads to the following trial function:

$$\psi(\mathbf{r},t) = \sqrt{\frac{N}{R_\rho(t)^2R_z(t)A_0[\xi(t)/R_\rho(t)]}}\left[\frac{\rho^2}{\rho^2+\xi(t)^2}\right]^{\frac{\ell}{2}} \times\sqrt{1-\frac{\rho^2}{R_\rho(t)^2}-\frac{z^2}{R_z(t)^2}} \times\exp\left[i\ell\varphi + iB_\rho(t)\frac{\rho^2}{2} + iC(t)\frac{\rho^4}{4} + iB_z(t)\frac{z^2}{2}\right], \tag{10}$$

with

$$A_0(\alpha) = \frac{2\pi^{3/2}(\ell)!}{15\alpha^{2\ell}\left(\frac{3}{2}+\ell\right)!}\left[(3+2\ell\alpha^2)\,{}_2F_1\left(\ell,1+\ell;\frac{5}{2}+\ell;-\frac{1}{\alpha^2}\right) - 2\ell(1+\alpha^2)\,{}_2F_1\left(1+\ell,1+\ell;\frac{5}{2}+\ell;-\frac{1}{\alpha^2}\right)\right], \tag{11}$$

where, for simplicity, we define $\alpha(t) = \xi(t)/R_\rho(t)$, ${}_pF_q(a_1,\ldots,a_p;b_1,\ldots,b_q;x)$ are the hypergeometric functions, $\xi(t)$ is the size of the vortex core, $R_\rho(t)$ is the condensate size in radial direction ($\hat{\rho}$), and $R_z(t)$ is the condensate size in axial direction ($\hat{z}$). The wave function (10) has an integration domain defined by $1-\frac{\rho^2}{R_\rho^2}-\frac{z^2}{R_z^2}\geqslant 0$, where the wave function is approximately an inverted parabola (TF shape), except for the central vortex. The trapping potential shape sets the condensate dimensions. To organize our calculations, we split the Lagrangian so that it is a sum $L=L_{\rm time}+L_{\rm kin}+L_{\rm pot}+L_{\rm int}$ of the following terms:

$$L_{\rm time}=\frac{i\hbar}{2}\int d^3\mathbf{r}\left[\psi^*(\mathbf{r},t)\frac{\partial\psi(\mathbf{r},t)}{\partial t}-\psi(\mathbf{r},t)\frac{\partial\psi^*(\mathbf{r},t)}{\partial t}\right]=-\frac{N\hbar}{2}\left(D_1\dot{B}_\rho R_\rho^2+D_2\dot{B}_zR_z^2+\frac{1}{2}D_3\dot{C}R_\rho^4\right),\tag{12}$$

$$\begin{aligned}L_{\rm kin}&=-\frac{\hbar^2}{2m}\int d^3\mathbf{r}[\nabla\psi^*(\mathbf{r},t)][\nabla\psi(\mathbf{r},t)]\\&=-\frac{N\hbar^2}{2m}\left[D_1B_\rho^2R_\rho^2+D_2B_z^2R_z^2+2D_3B_\rho CR_\rho^4+\ell^2R_\rho^{-2}(D_4+D_5)+D_6C^2R_\rho^6\right],\end{aligned}\tag{13}$$

$$L_{\rm pot}=-\frac{1}{2}m\omega_\rho^2\int d^3\mathbf{r}(\rho^2+\lambda^2z^2)\psi^*(\mathbf{r},t)\psi(\mathbf{r},t)=-\frac{N}{2}m\omega_\rho^2\left(D_1R_\rho^2+\lambda^2D_2R_z^2\right),\tag{14}$$

$$L_{\rm int}=-\frac{g}{2}\int d^3\mathbf{r}[\psi^*(\mathbf{r},t)\psi(\mathbf{r},t)]^2=-\frac{N^2gD_7}{2R_\rho^2R_z},\tag{15}$$

with the functions $D_i(\alpha)$ given by

$$D_1(\alpha)=A_0(\alpha)^{-1}\frac{2\pi^{3/2}(1+\ell)!}{21\alpha^{2\ell}\left(\frac{5}{2}+\ell\right)!}\left[(3+2\ell^2)_2F_1\left(\ell,2+\ell;\frac{7}{2}+\ell;-\frac{1}{\alpha^2}\right)-2\ell(1+\alpha^2)_2F_1\left(1+\ell,2+\ell;\frac{7}{2}+\ell;-\frac{1}{\alpha^2}\right)\right],\tag{16}$$

$$D_2(\alpha)=A_0(\alpha)^{-1}\frac{\pi^{3/2}(\ell)!}{4\alpha^{2\ell}\left(\frac{7}{2}+\ell\right)!}\left[(7+2\ell)_2F_1\left(\ell,1+\ell;\frac{7}{2}+\ell;-\frac{1}{\alpha^2}\right)-(5+2\ell)_3F_2\left(\ell,1+\ell,\frac{7}{2}+\ell;\frac{5}{2}+\ell,\frac{9}{2}+\ell;-\frac{1}{\alpha^2}\right)\right],\tag{17}$$

$$D_3(\alpha)=A_0(\alpha)^{-1}\frac{2\pi^{3/2}(2+\ell)!}{27\alpha^{2\ell}\left(\frac{7}{2}+\ell\right)!}\left[(3+2\ell)_2F_1\left(\ell,3+\ell;\frac{9}{2}+\ell;-\frac{1}{\alpha^2}\right)-2\ell(1+\alpha^2)_2F_1\left(1+\ell,3+\ell;\frac{9}{2}+\ell;-\frac{1}{\alpha^2}\right)\right],\tag{18}$$

$$D_4(\alpha)=A_0(\alpha)^{-1}\frac{2\pi^{3/2}(\ell-1)!}{3\alpha^{2\ell}\left(\frac{1}{2}+\ell\right)!}\left[(1-2\ell\alpha^2)_2F_1\left(\ell,2+\ell;\frac{3}{2}+\ell;-\frac{1}{\alpha^2}\right)+2\ell(1+\alpha^2)_2F_1\left(1+\ell,2+\ell;\frac{3}{2}+\ell;-\frac{1}{\alpha^2}\right)\right],\tag{19}$$

$$D_5(\alpha)=A_0(\alpha)^{-1}\frac{2\pi^{3/2}(\ell-1)!}{9\alpha^{2\ell}\left(\frac{1}{2}+\ell\right)!}\left[(3+2\ell\alpha^2)_2F_1\left(\ell,\ell;\frac{3}{2}+\ell;-\alpha^2\right)-2\ell(1+\alpha^2)_2F_1\left(\ell,1+\ell;\frac{3}{2}+\ell;-\frac{1}{\alpha^2}\right)\right],\tag{20}$$

$$D_6(\alpha)=A_0(\alpha)^{-1}\frac{2\pi^{3/2}(3+\ell)!}{33\alpha^{2\ell}\left(\frac{9}{2}+\ell\right)!}\left[(3+2\ell\alpha^2)_2F_1\left(\ell,4+\ell;\frac{11}{2}+\ell;-\frac{1}{\alpha^2}\right)-2\ell(1+\alpha^2)_2F_1\left(1+\ell,4+\ell;\frac{11}{2}+\ell;-\frac{1}{\alpha^2}\right)\right],\tag{21}$$

$$D_7(\alpha)=A_0(\alpha)^{-2}\frac{2\pi^{3/2}(2\ell)!}{\alpha^{4\ell}\left(\frac{7}{2}+\ell\right)!}{}_2F_1\left(2\ell,1+2\ell;\frac{9}{2}+2\ell;-\frac{1}{\alpha^2}\right).\tag{22}$$

For simplicity we can scale the variational parameters of the Lagrangian as well as the time in order to make them dimensionless,

$$\begin{aligned}&R_\rho(t)\to a_{\rm osc}r_\rho(t),\quad R_z(t)\to a_{\rm osc}r_z(t),\quad \xi(t)\to a_{\rm osc}r_\xi(t),\quad B_\rho(t)\to a_{\rm osc}^{-2}\beta_\rho(t),\\&B_z(t)\to a_{\rm osc}^{-2}\beta_z(t),\quad C(t)\to a_{\rm osc}^{-4}\zeta(t),\quad t\to\omega_\rho^{-1}\tau,\end{aligned}$$

where the harmonic-oscillator length is $a_{\rm osc}=\sqrt{\hbar/m\omega_\rho}$ and the dimensionless interaction parameter is $\gamma=Na_s/a_{\rm osc}$. Thus the Lagrangian becomes

$$L=-\frac{N\hbar\omega_\rho}{2}\left[D_1r_\rho^2\left(\dot{\beta}_\rho+\beta_\rho^2+1\right)+D_2r_z^2\left(\dot{\beta}_z+\beta_z^2+\lambda^2\right)+D_3r_\rho^4\left(\frac{1}{2}\dot{\zeta}+2\beta_\rho\zeta\right)+\ell^2r_\rho^{-2}(D_4+D_5)+D_6\zeta^2r_\rho^6+D_7\frac{4\pi\gamma}{r_\rho^2r_z}\right].\tag{23}$$

The Euler-Lagrange equations,

$$\frac{d}{dt}\left(\frac{\partial L}{\partial \dot{q_i}}\right) - \frac{\partial L}{\partial q_i} = 0, \tag{24}$$

for each one of the six variational parameters from Lagrangian (23) lead to the six differential equations:

$$\beta_\rho - \frac{\dot{r_\rho}}{r_\rho} - \frac{D_1'\dot{\alpha}}{2D_1} + \frac{D_3 r_\rho^2 \zeta}{D_1} = 0, \tag{25}$$

$$\beta_z - \frac{\dot{r_z}}{r_z} - \frac{D_2'\dot{\alpha}}{2D_2} = 0, \tag{26}$$

$$\zeta - \frac{D_3\dot{r_\rho}}{D_6 r_\rho} - \frac{D_3\dot{\alpha}}{4D_6 r_\rho^2} + \frac{D_3\beta_\rho}{D_6 r_\rho^2} = 0, \tag{27}$$

$$D_1 r_\rho(\dot{\beta_\rho} + \beta_\rho^2 + 1) + D_3 r_\rho^3(\dot{\zeta} + 4\beta_\rho\zeta) - \frac{\ell^2}{r_\rho^3}(D_4 + D_5) + 3D_6\zeta^2 r_\rho^5 - D_7\frac{4\pi\gamma}{r_\rho^3 r_z} = 0, \tag{28}$$

$$D_2 r_z\left(\dot{\beta_z} + \beta_z^2 + \lambda^2\right) - D_7\frac{2\pi\gamma}{r_\rho^2 r_z^2} = 0, \tag{29}$$

$$D_1' r_\rho^2(\dot{\beta_\rho} + \beta_\rho^2 + 1) + D_2' r_z^2\left(\dot{\beta_z} + \beta_z^2 + \lambda^2\right) + D_3' r_\rho^4\left(\frac{1}{2}\dot{\zeta} + 2\beta_\rho\zeta\right) + \frac{\ell^2}{r_\rho^2}(D_4' + D_5') + D_6'\zeta^2 r_\rho^6 - D_7'\frac{4\pi\gamma}{r_\rho^2 r_z} = 0. \tag{30}$$

Solving these equations for the parameters in the wave-function phase, we have

$$\beta_\rho = \frac{\dot{r_\rho}}{r_\rho} + F_1\dot{\alpha}, \tag{31}$$

$$\beta_z = \frac{\dot{r_z}}{r_z} + F_2\dot{\alpha}, \tag{32}$$

$$\zeta = F_3\frac{\dot{\alpha}}{r_\rho^2}, \tag{33}$$

where

$$F_1 = \frac{D_3' D_3 - 2D_1' D_6}{4\left(D_3^2 - D_1 D_6\right)}, \tag{34}$$

$$F_2 = \frac{D_2'}{2D_2}, \tag{35}$$

$$F_3 = \frac{2D_1' D_3 - D_1 D_3'}{4\left(D_3^2 - D_1 D_6\right)}. \tag{36}$$

Replacing (31), (32), and (33) into Eqs. (28), (29), and (30), we reduce our six coupled equations to only three, which are given by

$$D_1(\ddot{r_\rho} + r_\rho) + G_1 r_\rho\ddot{\alpha} + G_2 r_\rho\dot{\alpha}^2 + G_3\dot{r_\rho}\dot{\alpha} - G_4\frac{\ell^2}{r_\rho^3} - D_7\frac{4\pi\gamma}{r_\rho^3 r_z} = 0, \tag{37}$$

$$D_2(\ddot{r_z} + \lambda^2 r_z) + G_5 r_z\ddot{\alpha} + G_6 r_z\dot{\alpha}^2 + G_7\dot{r_z}\dot{\alpha} - D_7\frac{2\pi\gamma}{r_\rho^2 r_z^2} = 0, \tag{38}$$

$$D_1' r_\rho(\ddot{r_\rho} + r_\rho) + D_2' r_z(\ddot{r_z} + \lambda^2 r_z) + \left(G_8 r_\rho^2 + G_9 r_z^2\right)\ddot{\alpha} + \left(G_{10} r_\rho^2 + G_{11} r_z^2\right)\dot{\alpha}^2 + (G_{12} r_\rho\dot{r_\rho} + G_{13} r_z\dot{r_z})\dot{\alpha} + G_{14}\frac{\ell^2}{r_\rho^2} + D_7'\frac{4\pi\gamma}{r_\rho^2 r_z} = 0, \tag{39}$$

with

$$G_1 = D_1 F_1 + D_3 F_3, \tag{40}$$

$$G_2 = D_1\left(F_1^2 + F_1'\right) + D_3(4F_1 F_3 + F_3') + 3D_6 F_3^2, \tag{41}$$

$$G_3 = 2(D_1 F_1 + D_3 F_3) = 2G_1, \tag{42}$$

$$G_4 = D_4 + D_5, \tag{43}$$

$$G_5 = D_2 F_2, \tag{44}$$

$$G_6 = D_2\left(F_2^2 + F_2'\right), \tag{45}$$

$$G_7 = 2D_2 F_2 = 2G_5, \tag{46}$$

$$G_8 = D_1' F_1 + \tfrac{1}{2}D_3' F_3, \tag{47}$$

$$G_9 = D_2' F_2, \tag{48}$$

$$G_{10} = D_1'\left(F_1^2 + F_1'\right) + D_3'\left(\tfrac{1}{2}F_3' + 2F_1 F_3\right) + D_6' F_3^2, \tag{49}$$

$$G_{11} = D_2'\left(F_2^2 + F_2'\right), \tag{50}$$

$$G_{12} = 2D_1' F_1 + D_3' F_3, \tag{51}$$

$$G_{13} = 2D_2' F_2 = 2G_9, \tag{52}$$

$$G_{14} = D_4' + D_5'. \tag{53}$$

The terms $D_1 r_\rho$, $D_2\lambda^2 r_z$, $D_1' r_\rho^2$, and $D_2' r_z^2$ come from the trapping term L_{pot}, which can be neglected in the case of a freely expanding condensate. The parameter γ indicates the terms generated by the atomic interaction potential, while the fractions proportional to r_ρ^{-2} and r_ρ^{-3} come from the kinetic-energy contribution due to the presence of the vortex with charge ℓ. The remaining factors represent the coupling between the outer dimensions of the condensate and the vortex core.

Making the velocities ($\dot{r_\rho}, \dot{r_z}, \dot{\alpha}$) and accelerations ($\ddot{r_\rho}, \ddot{r_z}, \ddot{\alpha}$) equal to zero leads to the equations for the stationary solution:

$$D_1 r_{\rho 0} = G_4\frac{\ell^2}{r_{\rho 0}^3} + D_7\frac{4\pi\gamma}{r_{\rho 0}^3 r_{z0}}, \tag{54}$$

$$D_2\lambda^2 r_{z0} = D_7\frac{2\pi\gamma}{r_{\rho 0}^2 r_{z0}^2}, \tag{55}$$

$$D_1' r_{\rho 0}^2 + D_2'\lambda^2 r_{z0}^2 = -G_{14}\frac{\ell^2}{r_{\rho 0}^2} - D_7'\frac{4\pi\gamma}{r_{\rho 0}^2 r_{z0}}, \tag{56}$$

where r_ρ, r_z, and r_ξ take their respective equilibrium values $r_{\rho 0}$, r_{z0}, and $r_{\xi 0}$. We apply Newton's method to solve the coupled stationary equations (54)–(56). The value of the atomic interaction parameter used from now on in this paper is $\gamma = 800$, which is close to the value used in rubidium experiments [25].

IV. COLLECTIVE EXCITATIONS

For small deviations from the equilibrium configuration, we assume $r_\rho(t) \to r_{\rho 0} + \delta\rho(t)$, $r_z(t) \to r_{z0} + \delta z(t)$, and $\alpha(t) \to \alpha_0 + \delta\alpha(t)$, and neglect all terms of order 2 or higher in (37)–(39). This leads to the linearized matrix equation

$$\begin{pmatrix} D_1 & 0 & G_1 r_{\rho 0} \\ 0 & D_2 & G_5 r_{z0} \\ D_1' r_{\rho 0} & D_2' r_{z0} & G_8 r_{\rho 0}^2 + G_9 r_{z0}^2 \end{pmatrix} \begin{pmatrix} \ddot{\delta\rho} \\ \ddot{\delta z} \\ \ddot{\delta\alpha} \end{pmatrix}$$

$$+ \begin{pmatrix} D_1 + 3G_4 \frac{\ell^2}{r_{\rho 0}^4} + D_7 \frac{12\pi\gamma}{r_{\rho 0}^4 r_{z0}} & D_7 \frac{4\pi\gamma}{r_{\rho 0}^3 r_{z0}^2} & D_1' r_{\rho 0} - G_4' \frac{\ell^2}{r_{\rho 0}^3} - D_7' \frac{4\pi\gamma}{r_{\rho 0}^3 r_{z0}} \\ D_7 \frac{4\pi\gamma}{r_{\rho 0}^3 r_{z0}^2} & D_2 \lambda^2 + D_7 \frac{4\pi\gamma}{r_{\rho 0}^2 r_{z0}^3} & D_2' \lambda^2 r_{z0} - D_7' \frac{2\pi\gamma}{r_{\rho 0}^2 r_{z0}^2} \\ 2D_1' r_{\rho 0} - 2G_{14} \frac{\ell^2}{r_{\rho 0}^3} - D_7' \frac{8\pi\gamma}{r_{\rho 0}^3 r_{z0}} & 2D_2' \lambda^2 r_{z0} - D_7' \frac{4\pi\gamma}{r_{\rho 0}^2 r_{z0}^2} & D_1'' r_{\rho 0}^2 + D_2'' \lambda^2 r_{z0}^2 + G_{14}' \frac{\ell^2}{r_{\rho 0}^2} + D_7'' \frac{4\pi\gamma}{r_{\rho 0}^2 r_{z0}} \end{pmatrix} \begin{pmatrix} \delta\rho \\ \delta z \\ \delta\alpha \end{pmatrix} = 0, \quad (57)$$

which defines the matrices M and V, appearing in Eq. (2). Solving the characteristic equation,

$$\det(M^{-1}V - \varpi^2 I) = 0, \quad (58)$$

results in the frequencies of the collective modes of oscillation. Now the determinants $\det M$ and $\det V$ are both positive for $\ell = 1$. This means that a trapped condensate with a central singly charged vortex is described by a stable state. Since (58) is a cubic equation of ϖ^2, we have three pairs of frequencies $\pm\varpi_n$ $(n = z,\rho,\xi)$. There are three frequencies ϖ_n and four modes of oscillation in total, of which only three modes can be simultaneously observed depending on the anisotropy λ of harmonic potential as shown in Fig. 2. Among these four modes, two of them represent monopole oscillations, while the other two represent quadrupole oscillations of the atomic cloud. The B_1 mode [Fig. 3(a)] is characterized by having all condensate components r_i $(i = z,\rho,\xi)$ oscillating in phase; however, B_2 mode [Fig. 3(c)] presents r_ξ oscillating out of phase with r_ρ and r_z. The Q_1 mode [Fig. 3(b)] shows that r_z oscillation is out of phase with r_ξ and r_ρ, which are in phase with each other. However, in Q_2 mode [Fig. 3(d)] the oscillations of r_z and r_ξ are in phase with each other, with the r_ρ oscillation being out of phase with them. Extrapolating to an ideal situation where $\gamma = 0$, the equations of motion (37)–(39) can be decoupled. This way, the ϖ_z (lower frequency) represents only a r_z oscillation, ϖ_ρ (middle frequency) represents only a r_ρ oscillation, and ϖ_ξ (upper frequency) represents only a r_ξ oscillation.

In order to validate our results (Fig. 4), numerical simulations were performed using a direct simulation of GPE based on the Fourier spectral method, where the Fourier components of $\psi(\mathbf{r},t)$ were computed using fast Fourier transformations [26]. As the initial condition, we considered a small perturbation to the equilibrium configuration. By Fourier transforming the expectation value $\langle\rho^2\rangle$, it was possible to reproduce the excitation spectrum. Frequency values ϖ_n in the variational calculations differ from numerical values by less than 1%.

In Fig. 2(a), for $0.1 \leqslant \lambda \leqslant 1$, there exist two Q_2-like modes. The difference between them comes from the fact that vortex-core oscillation amplitude is two orders of magnitude lower at the less energetic mode. The same happens when $\ell = 2$ [Fig. 2(b)], i.e., the vortex core is almost still for the lower frequency in the same interval of λ.

The solid lines in Fig. 2 correspond to the mode with largest amplitude for the vortex-core oscillations. As can be seen, the excitation frequency ϖ_ξ of this mode lowers as the vortex circulation increases. It means that the energy necessary to excite it will be lower if ℓ is increased. However, we must point out that our results apply only for the cases where $r_\xi \ll r_\rho$.

V. SCATTERING-LENGTH MODULATION

One of the mechanisms used for exciting collective modes is via modulation of the s-wave scattering length. This technique has been already applied to excite the lowest-lying quadrupole mode in a lithium experiment [1]. Therefore, we consider the

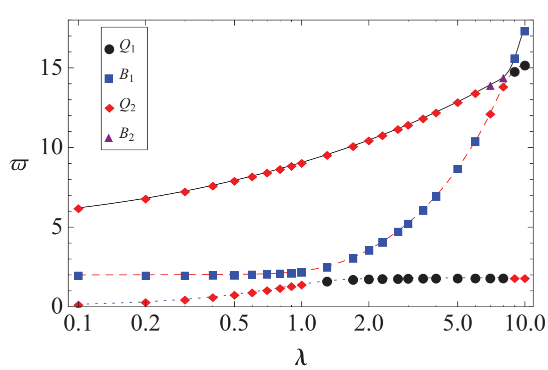

(a) $\ell = 1$

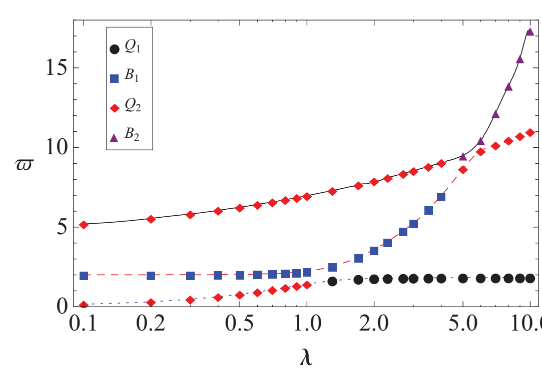

(b) $\ell = 2$

FIG. 2. (Color online) Oscillation frequencies as a function of trap anisotropy in a condensate containing a singly (a) and doubly (b) charged vortex at its center. Solid (black) line is ϖ_ξ, dashed (red) line is ϖ_ρ, and dotted (blue) line is ϖ_z.

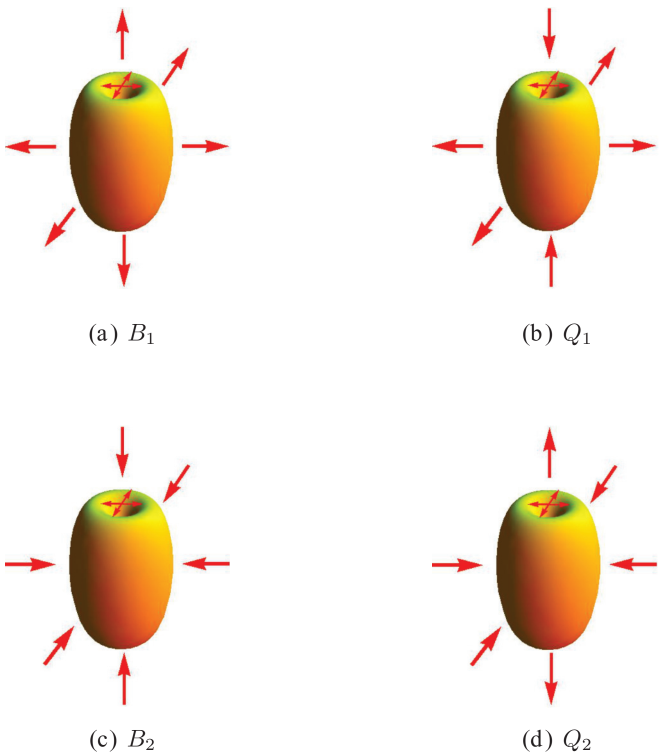

FIG. 3. (Color online) Schematic representation of collective modes. B_1 mode has all components oscillating in phase. B_2 mode has r_ξ oscillating out of phase with r_ρ and r_z. Q_1 mode has r_z oscillation out of phase with r_ξ and r_ρ. Q_2 mode has r_ρ oscillation out of phase with r_ξ and r_z.

time-dependent scattering length:

$$a_s(t) = a_0 + \delta a \cos(\Omega t). \tag{59}$$

This is equivalent to making $\gamma \to \gamma(\tau)$, thus giving

$$\gamma(\tau) = \gamma_0 + \delta\gamma \cos(\Omega\tau), \tag{60}$$

where γ_0 is the average value of the interaction parameter $\gamma(\tau)$, $\delta\gamma$ is the modulation amplitude, and Ω is the excitation

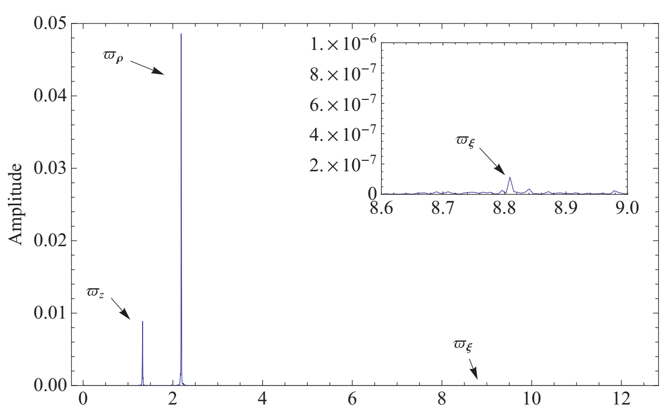

FIG. 4. (Color online) Fourier-transformed temporal evolution of $\langle\rho^2\rangle$ obtained from a numerical simulation of the GPE. We set $\gamma = 800$, $\ell = 1$, $\tilde{\mu} = 20.74$, and $\lambda = 0.9$. ϖ_n are the frequencies of the oscillation modes from less energetic (ϖ_z) to more energetic (ϖ_ξ). The analytical values are $\varpi_z = 1.317$, $\varpi_\rho = 2.166$, and $\varpi_\xi = 8.874$.

frequency. Substituting (60) into (57) and keeping only first-order terms ($\delta\rho$, δz, $\delta\alpha$, and $\delta\gamma$), we obtain a nonhomogeneous linear equation,

$$M\ddot{\delta} + V\delta = P \cos(\Omega\tau), \tag{61}$$

with

$$P = 2\pi\delta\gamma \begin{pmatrix} \frac{2D_7}{r_{\rho 0}^3 r_{z0}} \\ \frac{D_7}{r_{\rho 0}^2 r_{z0}^2} \\ \frac{D_7'}{r_{\rho 0}^2 r_{z0}} \end{pmatrix}. \tag{62}$$

A particular solution of (61) is

$$\delta_\gamma(\tau) = (M^{-1}V - \Omega^2)^{-1} M^{-1} P \cos(\Omega\tau). \tag{63}$$

Projecting the vector $\delta_\gamma(\tau)$ in the base δ_n ($n = z,\rho,\xi$) of the eigenvectors of the homogenous equation associated to Eq. (61), we obtain

$$\langle\delta_n|\delta_\gamma(\tau)\rangle = \frac{\langle\delta_n|M^{-1}P\rangle}{\varpi_n^2 - \Omega^2} \cos(\Omega\tau). \tag{64}$$

Since the scalar product $|\langle\delta_n|M^{-1}P\rangle|$ is always positive, it shows that specific collective modes can be excited using a scattering-length modulation with small amplitude $\delta\gamma$ and frequency Ω close to the one of the resonance frequency ϖ_n. In Fig. 5, we see the results from a numerical solution of

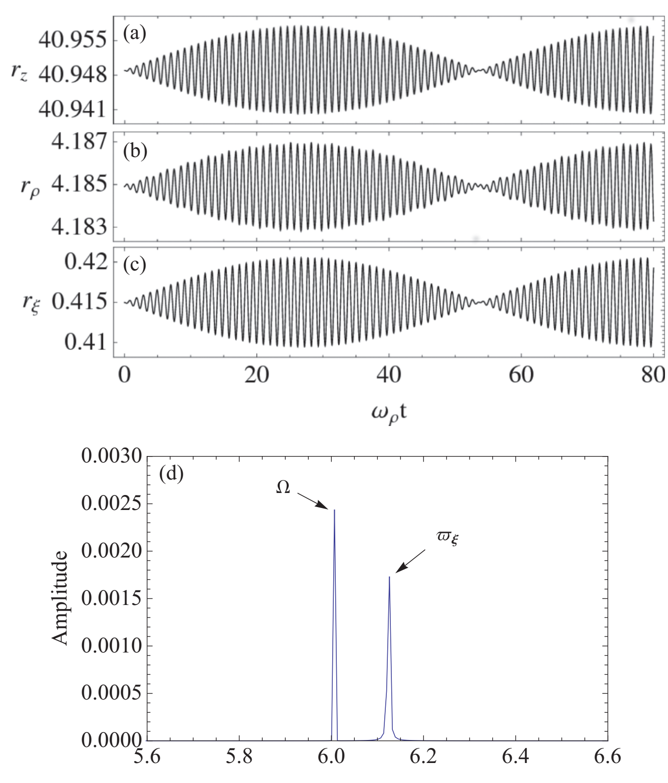

FIG. 5. (Color online) Numerical solution of Eqs. (37)–(39) with a time-dependent interaction $\gamma(\tau)$ (a), (b), and (c). (d) The excitation spectrum obtained from variational calculation, where $\varpi_\xi \approx 6.13$ is close to the value calculated in Eq. (58). We excited the collective mode Q_2 ($\varpi_\xi = 6.21$) of a condensate with a cigar shape ($\lambda = 0.1$, $\gamma_0 = 800$) via scattering-length modulation with amplitude $\delta\gamma = 0.4$ and frequency $\Omega = 6$.

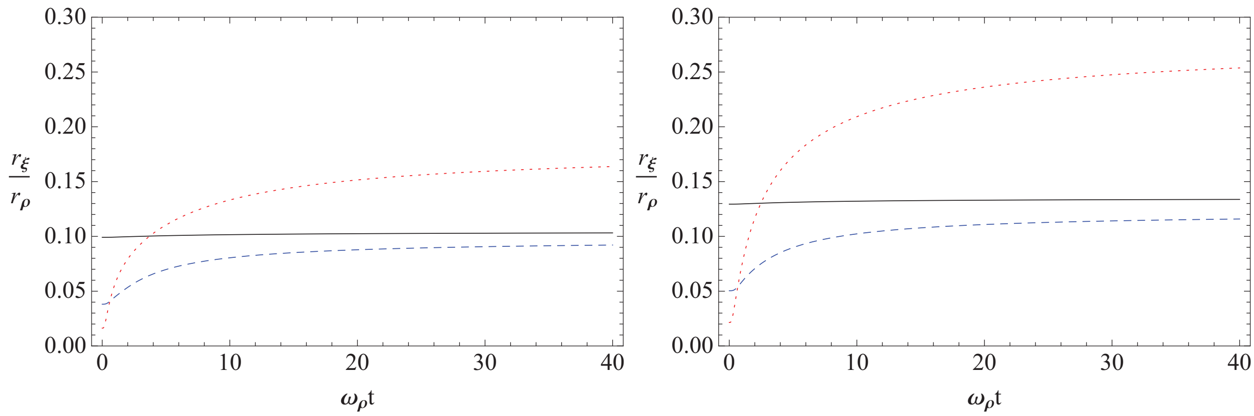

(a) $\ell = 1$ (b) $\ell = 2$

FIG. 6. (Color online) Ratio between vortex-core size and radial cloud size for different trap anisotropies while in free expansion. The solid (black) line corresponds to a prolate condensate ($\lambda = 0.1$), the dashed (blue) line to the isotropic case ($\lambda = 1$), and the dotted (red) line to an oblate condensate ($\lambda = 8$).

Eqs. (37)–(39) considering a time-dependent interaction $\gamma(\tau)$ according to Eq. (60). There we can see the beat behavior corresponding to a superposition of the frequencies $\Omega = 6$ and $\varpi_\xi = 6.13$.

VI. FREE EXPANSION

The time-of-flight pictures constitute the most common method to measure vortices in BEC. This method consists in switching off the magneto-optical trap and letting the atomic cloud expand freely for some time, typically ten milliseconds, and then taking a picture of the expanded cloud [5,27–31]. For this purpose, we use the equations of motion (37)–(39) without the terms arising from the harmonic potential, i.e.,

$$D_1\ddot{r_\rho} + G_1 r_\rho \ddot{\alpha} + G_2 r_\rho \dot{\alpha}^2 + G_3 \dot{r_\rho}\dot{\alpha} - G_4\frac{\ell^2}{r_\rho^3} - \frac{4D_7\gamma}{r_\rho^3 r_z} = 0, \tag{65}$$

$$D_2\ddot{r_z} + G_5 r_z \ddot{\alpha} + G_6 r_z \dot{\alpha}^2 + G_7 \dot{r_z}\dot{\alpha} - \frac{2D_7\gamma}{r_\rho^2 r_z^2} = 0, \tag{66}$$

$$\begin{aligned} &D_1' r_\rho \ddot{r_\rho} + D_2' r_z \ddot{r_z} + \left(G_8 r_\rho^2 + G_9 r_z^2\right)\ddot{\alpha} \\ &\quad + \left(G_{10} r_\rho^2 + G_{11} r_z^2\right)\dot{\alpha}^2 + (G_{12} r_\rho \dot{r_\rho} + G_{13} r_z \dot{r_z})\dot{\alpha} \\ &\quad + G_{14}\frac{\ell^2}{r_\rho^2} + \frac{4D_7'\gamma}{r_\rho^2 r_z} = 0, \end{aligned} \tag{67}$$

whose initial conditions are given by the stationary equations (54)–(56).

In Fig. 6, we have the ratio between vortex-core size (r_ξ) and radial cloud size (r_ρ) during free expansion for three different initial trap configurations. In general, the vortex core expands faster than the condensate at early times, going to the same rate of expansion at large times. The prolate condensate ($\lambda = 0.1$) has an almost constant ratio r_ξ/r_ρ during the entire expansion. For the isotropic ($\lambda = 1$) and oblate ($\lambda = 10$) cases, this ratio increases rapidly in the initial stage of the expansion until it converges to a constant value. These results agree with our previous work [24], where Fig. 6(b) could not be calculated since the authors considered the healing length as an approximation to the vortex-core radius which is only valid for $\ell = 1$. Such an agreement indicates the fact that, indeed, the vortex-core size is always close to the instantaneous healing length during the expansion. Moreover, since the radial component of the velocity field always points outwards from the cloud, the extra ρ^4 term in the wave-function phase is not necessary for a consistent description of the system.

VII. CONCLUSIONS

In this paper, we proposed a modification in the wave-function phase commonly used with the variational method which corrects the imaginary frequencies of collective modes when we have a parameter describing nonphysical vortex-core dynamics with $\ell = 1$.

Here we consider variational phase parameters corresponding to each parameter in wave-function amplitude, respectively. This way, we were able to describe the dynamics of both vortex core and the external dimensions of the condensate, which agrees with the numerical simulations of the GPE. Although we observe four modes of oscillation in total, only three of them can be simultaneously observed depending on the trap anisotropy. We also demonstrate that these oscillation modes can be excited by modulating the s-wave scattering length using the same experimental techniques as in Ref. [1].

Finally, we analyzed the time-of-flight dynamics of the vortex core with different circulations in order to complement the results in Ref. [24].

ACKNOWLEDGMENTS

We acknowledge financial support from the National Council for the Improvement of Higher Education (CAPES) and from the State of São Paulo Foundation for Research Support (FAPESP).

[1] S. E. Pollack, D. Dries, R. G. Hulet, K. M. F. Magalhães, E. A. L. Henn, E. R. F. Ramos, M. A. Caracanhas, and V. S. Bagnato, Phys. Rev. A **81**, 053627 (2010).
[2] S. Stringari, Phys. Rev. Lett. **77**, 2360 (1996).
[3] V. M. Pérez-García, H. Michinel, J. I. Cirac, M. Lewenstein, and P. Zoller, Phys. Rev. Lett. **77**, 5320 (1996).
[4] F. Dalfovo, S. Giorgini, L. P. Pitaevskii, and S. Stringari, Rev. Mod. Phys. **71**, 463 (1999).
[5] P. W. Courteille, V. S. Bagnato, and V. I. Yukalov, Laser Phys. **11**, 659 (2001).
[6] T. Busch, J. I. Cirac, V. M. Pérez-García, and P. Zoller, Phys. Rev. A **56**, 2978 (1997).
[7] Z. Zhang and W. V. Liu, Phys. Rev. A **83**, 023617 (2011).
[8] H. Heiselberg, Phys. Rev. Lett. **93**, 040402 (2004).
[9] A. Altmeyer, S. Riedl, C. Kohstall, M. J. Wright, R. Geursen, M. Bartenstein, C. Chin, J. H. Denschlag, and R. Grimm, Phys. Rev. Lett. **98**, 040401 (2007).
[10] M. Človečko, E. Gažo, M. Kupka, and P. Skyba, Phys. Rev. Lett. **100**, 155301 (2008).
[11] C. J. Pethick and H. Smith, *Bose-Einstein Condensation in Dilute Gases*, 2nd ed. (Cambridge University Press, Cambridge, UK, 2008).
[12] L. P. Pitaevskii and S. Stringari, *Bose-Einstein Condensation*, 1st ed. (Oxford University Press, New York, 2003).
[13] F. Zambelli and S. Stringari, Phys. Rev. Lett. **81**, 1754 (1998).
[14] A. Banerjee and B. Tanatar, Phys. Rev. A **72**, 053620 (2005).
[15] A. A. Svidzinsky and A. L. Fetter, Phys. Rev. A **62**, 063617 (2000).
[16] A. A. Svidzinsky and A. L. Fetter, Phys. Rev. Lett. **84**, 5919 (2000).
[17] M. Linn and A. L. Fetter, Phys. Rev. A **61**, 063603 (2000).
[18] V. M. Pérez-García and J. J. García-Ripoll, Phys. Rev. A **62**, 033601 (2000).
[19] L. Koens and A. M. Martin, Phys. Rev. A **86**, 013605 (2012).
[20] V. M. Pérez-García, H. Michinel, J. I. Cirac, M. Lewenstein, and P. Zoller, Phys. Rev. A **56**, 1424 (1997).
[21] A. A. Svidzinsky and A. L. Fetter, Phys. Rev. A **58**, 3168 (1998).
[22] D. H. J. O'Dell and C. Eberlein, Phys. Rev. A **75**, 013604 (2007).
[23] F. Dalfovo and M. Modugno, Phys. Rev. A **61**, 023605 (2000).
[24] R. P. Teles, F. E. A. dos Santos, M. A. Caracanhas, and V. S. Bagnato, Phys. Rev. A **87**, 033622 (2013).
[25] E. A. de Lima Henn, Ph.D. thesis, Universidade de São Paulo, São Carlos, 2008.
[26] G. R. Dennis, J. J. Hope, and M. T. Johnsson, Comput. Phys. Commun. **184**, 201 (2013).
[27] W. Ketterle, MIT Physics Annual (2001), pp. 44–49, http://web.mit.edu/physics/news/physicsatmit.html.
[28] E. A. L. Henn, J. A. Seman, E. R. F. Ramos, M. Caracanhas, P. Castilho, E. P. Olímpio, G. Roati, D. V. Magalhães, K. M. F. Magalhães, and V. S. Bagnato, Phys. Rev. A **79**, 043618 (2009).
[29] E. A. L. Henn, J. A. Seman, G. Roati, K. M. F. Magalhães, and V. S. Bagnato, Phys. Rev. Lett. **103**, 045301 (2009).
[30] F. Chevy, K. W. Madison, and J. Dalibard, Phys. Rev. Lett. **85**, 2223 (2000).
[31] B. P. Anderson, P. C. Haljan, C. E. Wieman, and E. A. Cornell, Phys. Rev. Lett. **85**, 2857 (2000).